

Ambient pressure colossal magnetocaloric effect tuned by composition in $Mn_{1-x}Fe_xAs$

ARIANA DE CAMPOS¹, DANIEL L ROCCO¹, ALEXANDRE MAGNUS G. CARVALHO¹, LUANA CARON¹, ADELINO A. COELHO¹, SERGIO GAMA^{1*}, LUZELI M. DA SILVA¹, FLÁVIO C. G. GANDRA¹, ADENILSON O. DOS SANTOS¹, LISANDRO P. CARDOSO¹, PEDRO J. VON RANKE² AND NILSON A. DE OLIVEIRA²

¹Instituto de Física Gleb Wataghin, Universidade Estadual de Campinas - UNICAMP, Caixa Postal 6165, 13083-970 Campinas, S. Paulo, Brazil

²Instituto de Física, Universidade do Estado do Rio de Janeiro—UERJ, Rua São Francisco Xavier, 524, 20550-013, RJ, Brazil

*e-mail: gama@ifi.unicamp.br

Published online: 3 September 2006; doi:10.1038/nmat1732

The magnetocaloric effect (MCE) is the basis for magnetic refrigeration, and can replace conventional gas compression technology due to its superior efficiency and environment friendliness^{1–3}. MCE materials must exhibit a large temperature variation in response to an adiabatic magnetic-field variation and a large isothermal entropic effect is also expected. In this respect, MnAs shows the colossal MCE, but the effect appears under high pressures⁴. In this work, we report on the properties of $Mn_{1-x}Fe_xAs$ that exhibit the colossal effect at ambient pressure. The MCE peak varies from 285 K to 310 K depending on the Fe concentration. Although a large thermal hysteresis is observed, the colossal effect at ambient pressure brings layered magnetic regenerators with huge refrigerating power closer to practical applications around room temperature.

The magnetocaloric effect (MCE) is important because of its potential applications in the domestic and industrial refrigeration markets. The effect is evaluated by two parameters, the adiabatic temperature variation ΔT_{ad} , and the isothermal entropic variation ΔS_{iso} for a material subjected to a magnetic-field variation¹. A large ΔS_{iso} is important, because it is proportional to the material refrigerating power¹. The possibility of tuning the transition temperature is also a key point to develop efficient active magnetic regenerator refrigerators^{1–3}.

For the materials exhibiting the conventional MCE, where the magnetic transitions are of the second-order type, the contribution to ΔS_{iso} is only of magnetic origin^{1–3,5}. On the other hand, when a first-order transition occurs, the MCE is giant^{6–10} and ΔS_{iso} also includes a considerable contribution from the lattice through the latent heat^{5,11,12}. Up to now, no material exhibiting either the conventional or the giant MCE (GMCE) shows an entropic effect surpassing the magnetic limit posed by the relation $R \ln(2J+1)$ (refs 1–3), where R is the gas constant and J is the total angular momentum of the magnetic ion.

Recently, we disclosed the colossal MCE (CMCE) in MnAs under pressure⁴, which exhibits a maximum ΔS_{iso} 2.6 times the magnetic limit for MnAs. To account for such a great value for ΔS_{iso} , we proposed a model where a large contribution to the MCE is extracted from the lattice by the field variation through

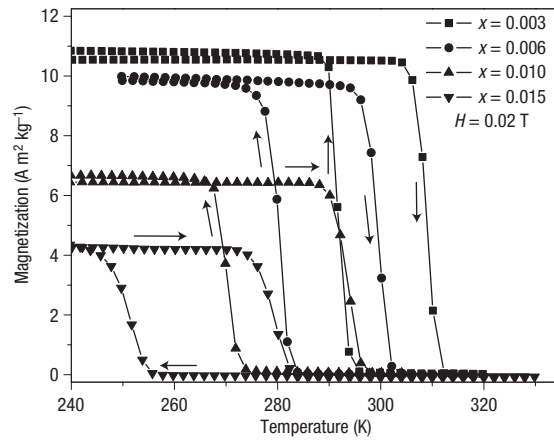


Figure 1 The effect on magnetization from Fe substitution for Mn in MnAs. Magnetization curves as a function of temperature for an applied magnetic field of 0.02 T (the lines are guides for the eye).

the strong magnetoelastic interaction present in MnAs^{4,13,14}. This lattice effect, however, is not to be mistaken as the latent heat lattice contribution^{11,12} observed in the case of the GMCE. In the case of the CMCE materials the latent heat contribution is only a fraction of the observed entropic effect⁴. The colossal effect is of prime importance for applications because of the huge potential refrigerating power of the material. In addition, tunable CMCE will allow the use of layered regenerators¹⁵ with overall refrigerating powers far greater than possible with materials exhibiting conventional or GMCE.

Other materials such as $Gd_5Ge_2Si_2$ (ref. 16), $MnFeP_{0.8}Ge_{0.2}$ (L. Caron *et al.*, to be published) and the manganite $La_{0.8}Sr_{0.2}MnO_3$ (ref. 17) exhibiting similar properties (for example, strong magnetoelastic interaction) were studied under pressure, but none showed the CMCE. Measurements for $La(Fe_{1-x}Si_x)_{13}H_y$ (ref. 18) show that pressure decreases the Curie temperature, T_C , and

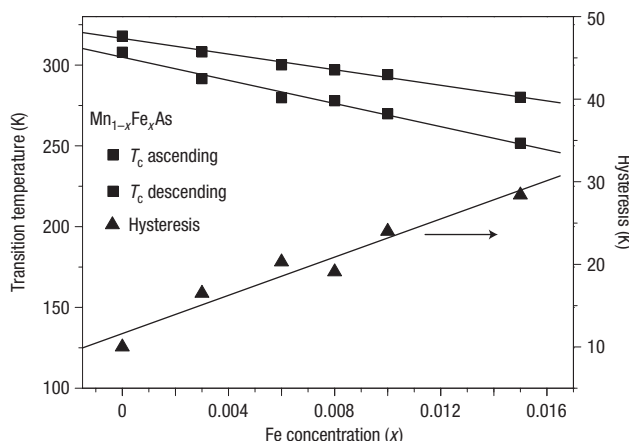


Figure 2 The effect on transition temperature and hysteresis from Fe substitution for Mn in MnAs. Linear variations of the transition temperature with increasing and decreasing temperature, and of the width of the thermal hysteresis as a function of Fe concentration. The lines are linear fits to the experimental data (symbols).

increases ΔS_{iso} , but the MCE remains in the giant effect range. We then focused our search on MnAs derivatives, obtained by doping it with several atoms, with two aims. One aim was to reduce hysteresis and the other was to obtain the same effect at lower or at ambient pressure. We studied substitutions of Sb for As, because these compounds exhibit the giant effect with small hysteresis, T_C is tuned by the Sb amount, and they have strong magnetoelastic interaction^{9,10}. Indeed, the compound $\text{MnAs}_{0.95}\text{Sb}_{0.05}$ showed the CMCE (A. de Campos *et al.*, to be published) with the same features observed in MnAs, both under pressure. We stress that on these substitutions, a low solubility of the dopants and the precipitation of a second phase (A. de C., A. A. C., S. G. and A. I. C. Persiano, presented in *First IIR Int. Conf. On Magnetic Refrigeration at Room Temperature* Montreux, Switzerland, 27–30 September 2005) are always observed.

We also studied substitutions in the Mn site in MnAs. We selected Fe due to the similarities between iron and manganese and their mutual solubility¹⁹, simplifying the doping process. Given the small difference in the atomic radii, we expected that the substitution of Fe for Mn should emulate the pressure effect observed in MnAs. Indeed, T_C shifts to lower temperatures (Fig. 1), the thermal hysteresis markedly increases (Fig. 2) and the saturation magnetization shows a sudden decrease (Fig. 3a) as x increases in $\text{Mn}_{1-x}\text{Fe}_x\text{As}$.

The entropic MCE was measured in the vicinity of the transition using the isothermal magnetization curves (Fig. 3b) and we found it to have the colossal character (where the entropy is above the entropy magnetic limit), even at ambient pressure (Fig. 4). It is clear that the introduction of Fe produces results similar to an applied hydrostatic pressure in MnAs. A drastic drop of the MCE is observed in $\text{Mn}_{1-x}\text{Fe}_x\text{As}$ for $x > 0.0125$ (Fig. 4), accompanied by a drop in M_s as well as by a change from ferromagnetic to antiferromagnetic-like behaviour²⁰ (Fig. 3a, $x = 0.0175$). We note that for the case of MnAs, the MCE completely disappears as pressure increases above a critical value⁴.

The behaviour and values of the refrigerating power for the Fe-doped compounds are similar to those observed for MnAs at ambient pressure. The difference is that the refrigerating power observed in the colossal effect is concentrated in a small temperature interval, meaning that for this small temperature

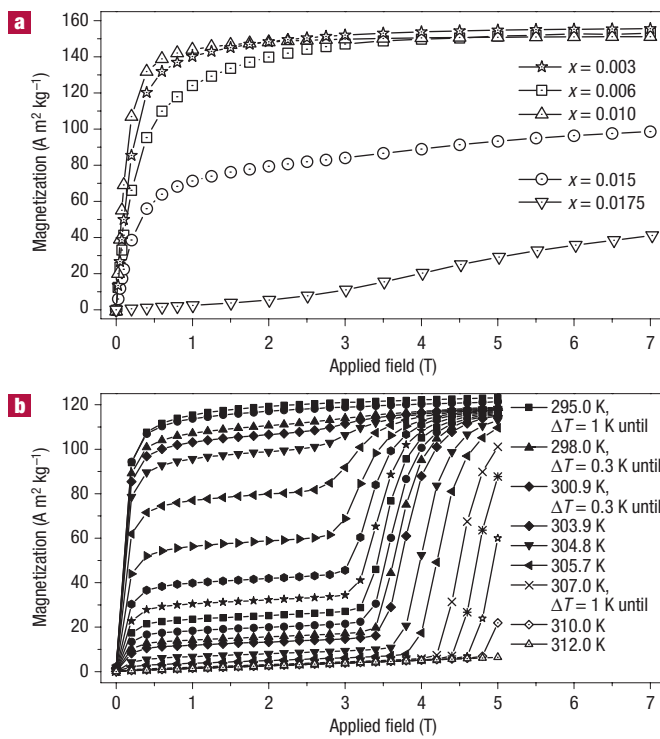


Figure 3 Behaviour of $\text{Mn}_{1-x}\text{Fe}_x\text{As}$ magnetization at low temperatures and around the Curie point. **a**, Magnetization of $\text{Mn}_{1-x}\text{Fe}_x\text{As}$ as a function of applied magnetic field and Fe content at 7 K, measured with increasing field. Note the onset of antiferromagnetic-like behaviour for $x > 0.015$. **b**, Isothermal magnetization curves around the magnetic transition for $x = 0.006$. The curves shown are for increasing field and temperature.

difference between a hot and a cold reservoir it is possible to extract a large amount of heat. This material is of particular importance as it exhibits the CMCE in the temperature range between 285 and 310 K. The design of layered active magnetic regenerators with large refrigerating power is favoured by the possibility of tuning T_C by the Fe concentration, in a relatively large temperature interval. It is just necessary to consider that each layer ‘works’ in a temperature interval centred at the peak of the CMCE.

The analysis of the Rietveld refinements confirmed the hexagonal NiAs-type structure for the ordered phase and the orthorhombic MnP-type structure for the paramagnetic phase. The Fe substitution for Mn leads to a decrease of the lattice parameters and of the unit cell volume, corroborating a correspondence between external pressure and chemical pressure (Fe concentration), for both phases. Values for an equivalent pressure for each Fe content were obtained using the P versus T_C relations established by Menyuk *et al.*²⁰. From these equivalent pressures and the unit cell volume contraction we estimated the equivalent compressibility of the doped compounds, obtaining an average value of $2.7 \times 10^{-11} \text{ Pa}^{-1}$, consistent with Menyuk’s value of $4.55 \times 10^{-11} \text{ Pa}^{-1}$ for MnAs (ref. 20).

An important question is whether the iron doping is just promoting a volumetric effect or if the electronic structure of the compound is also being altered (note that the colossal effect found in $\text{Gd}_5(\text{Si}_{1-x}\text{Ge}_x)_4$ (ref. 6) as a consequence of chemical pressure has no counterpart on Gd_5Ge_4 under external pressure (Z. Arnold, presented in *Course Held at the Physics Institute of the State University of Campinas—Unicamp January 2005*)). In fact, low-temperature specific heat measurements reveal the same electronic

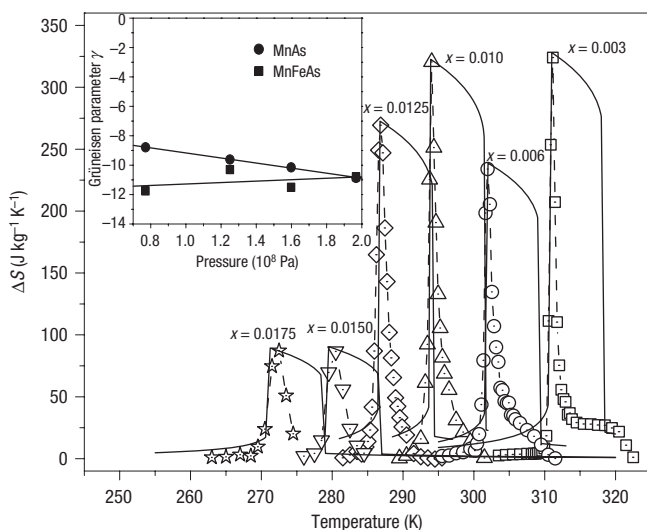


Figure 4 The colossal effect for $\text{Mn}_{1-x}\text{Fe}_x\text{As}$ as a function of temperature and Fe content for a magnetic field variation of 5 T. The measurements were carried out with increasing temperature. The symbols correspond to experimental data. The dashed lines through the experimental points are guides to the eye. The solid lines are the theoretical model results. The inset shows the Grüneisen parameters for the MnAs and $\text{Mn}_{1-x}\text{Fe}_x\text{As}$ compounds. The lines in the inset are linear fits to the experimental data.

coefficient for both MnAs and $\text{Mn}_{1-x}\text{Fe}_x\text{As}$, indicating that there is no alteration of the density of electronic states at the Fermi level caused by the presence of Fe. Applying the model previously proposed to explain the CMCE (ref. 13) in MnAs to this case (Fig. 4), we are able to reproduce the experimental data reasonably well. As is typical for the model, it provides a larger temperature window for the effect than the experiment. The calculation results show the Grüneisen parameters for $\text{Mn}_{1-x}\text{Fe}_x\text{As}$ to vary at a fairly slower rate ($0.49 \times 10^{-8} \text{ Pa}^{-1}$) than for MnAs ($-1.74 \times 10^{-8} \text{ Pa}^{-1}$) (Fig. 4, inset), besides a change of sign of this rate. This is an indication that the presence of Fe is causing more than just the chemical pressure. Nevertheless, T_C variation for the Fe-doped material obtained by application of external pressure is compatible with the value for pure MnAs ($1.75 \times 10^{-7} \text{ K Pa}^{-1}$ for $x = 0.003$, $1.69 \times 10^{-7} \text{ K Pa}^{-1}$ in average for all x and $1.64 \times 10^{-7} \text{ K Pa}^{-1}$ for $x = 0$). Therefore, the correspondence between pressure and Fe content in principle supports the idea that the main role of the Fe atoms is to cause a linear decrease of the unit cell volume. Nevertheless, further analysis should be carried out to clarify this aspect.

The discovery of the series of compounds $\text{Mn}_{1-x}\text{Fe}_x\text{As}$ with CMCE at ambient pressure and with transition temperatures tuned by the Fe content opens up the possibility of the construction of layered active magnetic regenerator refrigerators with refrigerating powers unthinkable up to now. They also operate in the temperature range from 310 K to 285 K, a very important temperature interval for domestic and industrial applications. This new material, together with others to be discovered with similar properties in a wider temperature span, can reshape the perspectives of practical applications of magnetic refrigeration technology in our society. An important matter to be addressed in future research of these materials is how to reduce or even eliminate the thermal hysteresis, which is still too large to allow direct use of this new material.

METHODS

The samples for this work were prepared using a method we developed that avoids the long reaction-sintering heat treatments reported in the literature^{9,10}. First, a mother Fe-Mn alloy was arc melted under argon atmosphere. Each compound was then prepared with all the Fe coming from the mother alloy plus the appropriate amounts of pure Mn and As to complete the 1:1 'MnAs' stoichiometry. All materials were in pieces, and the total amount of each sample was 5 g. The materials sealed in a quartz tube under vacuum were heat treated in a resistive furnace at 1,070 °C for 2 h to assure the melting and thorough mixing of the components, and were then quenched to room temperature. The tube containing the sample was then reheated to 800 °C for 48 h and subsequently water quenched to ambient temperature.

Samples were characterized by metallographic analyses, X-ray diffraction and magnetic measurements before the measurements to determine the MCE were carried out. All Fe-doped samples formed a single phase, as shown by both metallography and X-ray diffraction, and confirmed by the magnetization as a function of temperature for a 0.02 T applied magnetic field. Transition temperatures were determined through the minimum of the temperature derivative of the curves $M \times T$ for the 0.02 T applied field.

The MCE was measured using magnetic measurements obtained from a commercial superconducting quantum interference device magnetometer and numerically integrating the Maxwell relation $(\partial S / \partial H)|_T = (\partial M / \partial T)|_H$, where S is the total entropy of the material, M is its magnetization and H is the external applied magnetic field.

Received 18 March 2006; accepted 7 August 2006; published 3 September 2006.

References

1. Tishin, A. M. & Spichkin, I. *The Magnetocaloric Effect and its Applications* (Institute of Physics Publishing, Bristol, 2003).
2. Gschneidner, K. A. Jr, Pecharsky, V. K. & Tsokol, A. O. Recent developments in magnetocaloric materials. *Rep. Prog. Phys.* **68**, 1479–1539 (2005).
3. Brück, E. Developments in magnetocaloric refrigeration. *J. Phys. D Appl. Phys.* **38**, R381–R391 (2005).
4. Gama, S. *et al.* Pressure-induced colossal magnetocaloric effect in MnAs. *Phys. Rev. Lett.* **93**, 237202 (2004).
5. Pecharsky, V. K., Gschneidner, K. A. Jr, Pecharsky, A. O. & Tishin, A. M. Thermodynamics of the magnetocaloric effect. *Phys. Rev. B* **64**, 144406 (2001).
6. Pecharsky, V. K. & Gschneidner, K. A. Jr. Giant Magnetocaloric Effect in $\text{Gd}_5(\text{Si}_2\text{Ge}_{1-x})_4$. *Phys. Rev. Lett.* **78**, 4494–4497 (1997).
7. Tegus, O., Brück, E., Buschow, K. H. J. & de Boer, F. R. Transition-metal-based magnetic refrigerants for room-temperature applications. *Nature* **415**, 150–152 (2002).
8. Fujita, A., Fujieda, S., Hasegawa, Y. & Fukamichi, K. Itinerant-electron metamagnetic transition and large magnetocaloric effects in $\text{La}(\text{Fe}_{1-x}\text{Si}_x)_13$ compounds and their hydrides. *Phys. Rev. B* **67**, 104416–104418 (2003).
9. Wada, H. & Tanabe, Y. Giant magnetocaloric effect of $\text{MnAs}_{1-x}\text{Sb}_x$. *Appl. Phys. Lett.* **79**, 3302–3304 (2001).
10. Wada, H., Taniguchi, K. & Tanabe, Y. Extremely large magnetic entropy change of $\text{MnAs}_{1-x}\text{Sb}_x$ near room temperature. *Mater. Trans.* **43**, 73–77 (2002).
11. Pecharsky, V. K., Holm, A. P., Gschneidner, K. A. Jr & Rink, R. Massive magnetic-field-induced structural transformation in Gd_3Ge_4 and the nature of the first order transition. *Phys. Rev. Lett.* **91**, 197204 (2003).
12. Morellon, L. *et al.* Pressure enhancement of the giant magnetocaloric effect in $\text{Tb}_3\text{Si}_2\text{Ge}_2$. *Phys. Rev. Lett.* **93**, 137201 (2004).
13. von Ranke, P. J. *et al.* Theoretical description of the colossal entropic magnetocaloric effect: Application to MnAs. *Phys. Rev. B* **73**, 014415 (2006).
14. von Ranke, P. J., de Oliveira, N. A., Mello, C., Carvalho, A. M. G. & Gama, S. Analytical model to understand the colossal magnetocaloric effect. *Phys. Rev. B* **71**, 054410 (2004).
15. Richard, M. A., Rowe, A. M. & Chahine, R. Magnetic refrigeration: Single and multitemperature active magnetic regenerators experiments. *J. Appl. Phys.* **95**, 2146–2150 (2004).
16. Carvalho, A. M. G. *et al.* The magnetic and magnetocaloric properties of $\text{Gd}_3\text{Ge}_4\text{Si}_2$ compound under hydrostatic pressure. *J. Appl. Phys.* **97**, 10M320 (2005).
17. Rocco, D. L. *et al.* Magnetocaloric effect of $\text{La}_{0.8}\text{Sr}_{0.2}\text{MnO}_3$ compound under pressure. *J. Appl. Phys.* **97**, 10M317 (2005).
18. Fujita, A. & Fukamichi, K. Proc. First IIR Int. Conf. On Magnetic Refrigeration at Room Temperature (Montreux, Switzerland, 27–30 Sept. 2005) 201–209 (International Institute of Refrigeration, Paris, 2005).
19. Massalski, T. B. (ed.) in *Binary Alloy Phase Diagrams* 2nd edn (ASM International, Materials Park, 1990).
20. Menyuk, N., Kafalas, J. A., Dwight, K. & Goodenough, J. B. Effects of pressure on the magnetic properties of MnAs. *Phys. Rev.* **177**, 942–951 (1969).

Acknowledgements

The authors acknowledge financial support from Fapesp—Fundação de Amparo à Pesquisa do Estado de São Paulo, CNPq—Conselho Nacional de Desenvolvimento Científico e Tecnológico and from Capes—Coordenação de Aperfeiçoamento do Pessoal de Nível Superior. Correspondence and requests for materials should be addressed to S.G.

Competing financial interests

The authors declare that they have no competing financial interests.

Reprints and permission information is available online at <http://npg.nature.com/reprintsandpermissions/>